Instructors, Specialists

☐Instructors 487

☐Specialists 1,138

Lung Cancer 肺癌

☐Lung Cancer Patients 肺癌
60,000/year

☐Rate of Surgery
50%

☐Lung Cancer Surgery 手術
30,000/year

Lung Cancer Surgery

☐Surgery 手術	30,000
☐Surgery per Surgeon	100
☐No. of Specialists 專門醫	300
☐Working Period	35 歲－55 歲
☐Newcomer 新專門醫	15

General Thoracic Surgical Club

- General Thoracic Surgeons
  - ☐ Lung Cancer + benign
  - ☐ Esophageal Cancer + benign
- 300 American Members
- 50 International Members

Japan vs. China

☐Population 人口
- ■ Japan 日本 120,000,000
- ■ China 中國 1,300,000,000

☐Lung Cancer Surgeons
- ■ Japan 日本 300
- ■ China 中國 3,000

Mission of Association 服務

- Practice 臨床
  - Contribution to Community
    - Information
- Education 教育
- Research 研究
  - Advancement of Thoracic Surgery

JJCLCR 肺癌聯合登録委員会

Japanese Joint Committee of Lung Cancer Registry

- The Japanese Association for **Chest Surgery**
- The Japan **Lung Cancer** Society
- The Japanese **Respiratory** Society

A Japanese Lung Cancer Registry Study

REGISTRY:

- Surgically resected primary lung neoplasms only in **1994** from **303 teaching hospitals** in Japan
- Neoplasms including lung cancer of all histologic types and low-grade malignancy
- Exclusion of exploration case and recurrent tumor
- A retrospective questionnaire on 27 items

A Japanese Lung Cancer Registry Study

7,488 pts. registered from 303 teaching hospitals

- **15 ineligible reports**
- **749 histologies of SCLC or low-grade malignancy**

6,644 pts. with non-small cell histology (89.9%) for this analysis

Rare Histological Type

☐Small cell carcinoma	248
☐Carcinoid	73
☐Adenoid cystic carcinoma	4
☐Mucoepidermoid carcinoma	19

OVERALL SURVIVAL 6,644 NSCLC

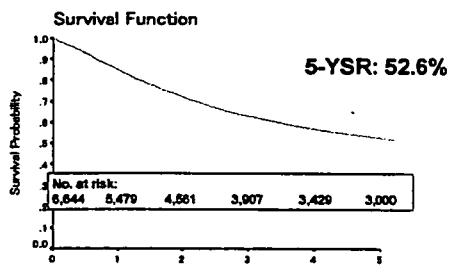

SURVIVAL by c-STAGE

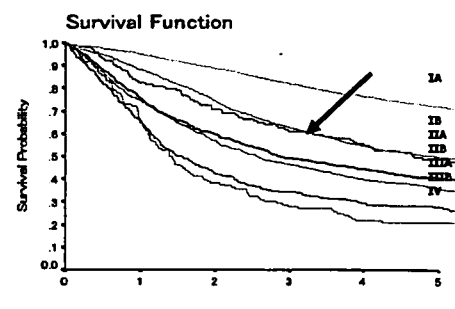

DIFFERENCE between STAGES:
c-STAGE

c-Stage	n	5-YSR(%)	Difference (P)
IA	2,423	72.1	
IB	1,542	49.9	0.0000
IIA	150	48.7	0.4969
IIB	746	40.6	0.0458
IIIA	1,270	35.8	0.0439
IIIB	366	28.0	0.0000
IV	147	20.8	0.1577

2007/1/21 第一届 中國胸科外科論議 上海 下午25/35

Lung Cancer (2005) 50:227-234

Prognosis of 6644 resected non-small cell lung cancers in Japan: A Japanese lung cancer registry study

The Japanese Joint Committee of Lung Cancer Registry

2007/1/21 第一届 中國胸科外科論議 上海 下午26/35

SURVIVAL CURVES BY GENDER

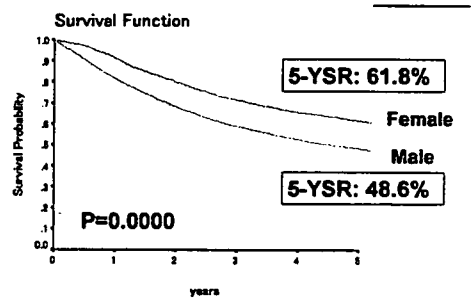

2007/1/21 第一届 中國胸科外科論議 上海 下午27/35

SURVIVAL CURVES BY AGE

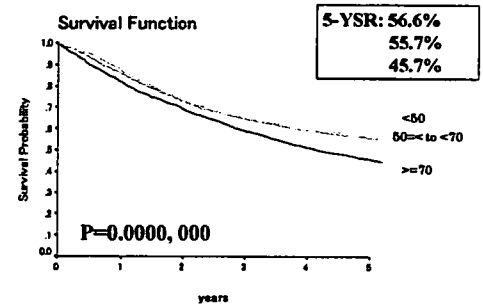

2007/1/21 第一届 中國胸科外科論議 上海 下午28/35

SURVIVAL CURVES BY HISTOLOGY

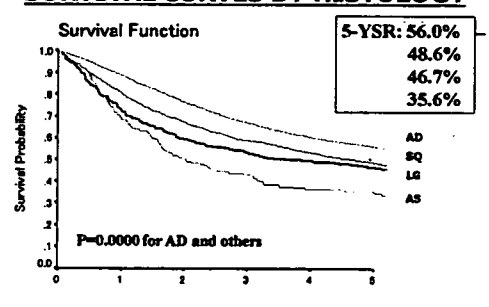

2007/1/21 第一届 中國胸科外科論議 上海 下午29/35

IASLC Staging Project
NSCLC and SCLC Cases 2 JUN 2004

	Total	Included	Primary Reason Excluded			
			Time Frame	Surv -Data	Stage	Total
Total	48,445	43,455	523	591	3,876	4,990
Japan	7,256	7,143	6	99	8	113
Korea	1,084	840	244	0	0	244
MacCallum	203	183	20	0	0	20
U Sydney	2,546	1,609	0	0	3	937
Amsterdam	13,895	11,346	0	0	2,549	2,549
ELCWP	2,068	2,067	0	1	0	1
Flemish	6,769	5,189	0	442	1,129	1,571
Gdansk	1,262	1,247	0	2	13	15
Grenoble	906	692	178	3	33	214

(table continues next slide)

2007/1/21 第一届 中國胸科外科論議 上海 下午30/35

IASLC Staging Project
NSCLC and SCLC Cases
21 JUN 2004

	Total	Included	Primary Reason Excluded			
			Time Frame	Surv Data	Stage	Total
Heidelberg	5,391	5,391	0	0	0	0
Jules Bordet	746	697	5	23	21	49
Perugia	110	94	5	3	8	16
Spain	2,991	2,941	0	18	32	50
Torino	1,006	918	65	0	23	88
NCIC	255	255	0	0	0	0
SWOG/BLOT	2,900	2,843	0	0	57	57
Total	48,445	43,455	523	591	3,876	4,990

(table continued from previous slide)

IASLC Staging Project
Clinical Stage – NSCLC (Broad Inclusion Criteria)

	Total	0	1A	1B	2A	2B	3A	3B	4
Total	31580	24	4348	5726	249	2730	4960	5168	8375
Japan	6875	11	2499	1591	141	800	1293	384	156
MacCallum	183	0	8	22	3	19	78	53	0
Amsterdam	8500	0	713	1194	30	395	1111	1728	3329
ELCWP	1489	0	14	5	1	63	340	281	785
Flemish	4699	3	374	871	37	365	826	907	1316
Grenoble	178	0	31	59	3	19	34	23	9
Heidelberg	4460	0	193	469	30	545	946	1215	1062
Jules Bordet	550	0	10	31	0	14	60	97	338
Spain	2570	10	508	1423	0	364	90	137	40
NCIC	35	0	0	0	0	0	35	0	0
SWOG/BLOT	2041	0	0	61	4	146	147	343	1340

IASLC Staging Project - NSCLC Database
Nodal station

	cTNM	pTNM	Size of lesion	T-descriptors (cT or pT)	Complete-ness of Resection	Nodal Stations	T4 Subset (cT or pT)	
							Malignant effusions (+/-)	Satellite Nodules (+/-)
Total	31,490	20,622	11,314	16,857	14,270	8,144	3,043	1456
Japan	6,875	6,753	6,857	6,899	6,744	6,899	768	916
Korea		631	776					120
MacCallum	183		136					
U Sydney		1,591		1,591			172	
Amsterdam	8,500	2,266						
ELCWP	1,489						132	
Flemish	4,699	1,419		4,731	1,374		1,133	
Gdansk	1	1239						
Grenoble	178	648						
Heidelberg	4,460	2,060			2,060			
Jules Bordet	550	11					102*	
Perugia		94	91					
Spain	2,570	2,889	2,558	2,890	2,876		456	458
Torino		895	892	177	894	895	6	26
NCIC	35					35		
SWOG/BLOT	1951	124		362	322	315	200	35

3 Poles in the World

- Europe
- America
- Asia
  - China
  - Japan
  - Korea

謝 謝

Fluorine 18–tagged fluorodeoxyglucose positron emission tomographic scanning to predict lymph node metastasis, invasiveness, or both, in clinical T1 N0 M0 lung adenocarcinoma

Hiroaki Nomori, MD, PhD[a]
Kenichi Watanabe, MD[a]
Takashi Ohtsuka, MD[a]
Tsuguo Naruke, MD, PhD[a]
Keiichi Suemasu, MD, PhD[a]
Toshiaki Kobayashi, MD, PhD[b]
Kimiichi Uno, MD, PhD[c]

See related editorial on page 341.

Objective: We sought to predict lymph node metastasis and tumor invasiveness in clinical T1 N0 M0 lung adenocarcinomas, and we measured fluorodeoxyglucose uptake on positron emission tomography.

Methods: Fluorodeoxyglucose positron emission tomography was performed on 44 patients with adenocarcinomas of 1 to 3 cm in size clinically staged as T1 N0 M0 before major lung resection with lymph node dissection. Fluorodeoxyglucose uptake was evaluated by using the contrast ratio between the tumor and contralateral healthy lung tissue. Lymphatic and vascular invasion within tumors, pleural involvement, and grade of histologic differentiation were examined.

Results: The pathologic tumor stage was T1 N0 M0 in 36 patients, and a more advanced stage was found in 8 patients. Although all 22 adenocarcinomas with a contrast ratio of less than 0.5 in fluorodeoxyglucose uptake were pathologic T1 N0 M0 tumors, 8 (36%) of 22 with a contrast ratio of 0.5 or greater were of a more advanced stage than T1 N0 M0, with the difference being significant ($P = .002$). Adenocarcinomas with a contrast ratio of less than 0.5 showed less lymphatic and vascular invasion and less pleural involvement than those with a contrast ratio of 0.5 or greater ($P = .006$, $P = .004$, and $P = .02$, respectively). The grade of histologic differentiation was well differentiated in 19 of 22 adenocarcinomas with a contrast ratio of less than 0.5 (86%), which was a greater frequency than the 4 (18%) of 22 adenocarcinomas with a contrast ratio of 0.5 or greater ($P < .001$).

Conclusion: Clinical T1 N0 M0 lung adenocarcinomas with a contrast ratio of less than 0.5 usually did not have lymph node metastasis, had less tumor involvement of vessels or pleura, and were more frequently well differentiated than those with a contrast ratio of 0.5 or greater. Limited lung resection could be indicated, lymph node dissection or mediastinoscopy could be reduced, or both in this type of adenocarcinoma.

From the Department of Thoracic Surgery,[a] Saiseikai Central Hospital, Tokyo, Japan; the Endoscopy Division,[b] National Cancer Center Hospital, Tokyo, Japan; and Nishidai Clinic,[c] Tokyo, Japan.

This work was supported in part by a Grant-in-Aid from the Ministry of Health, Labor, and Welfare of Japan.

Received for publication Dec 17, 2003; revisions requested Feb 12, 2004; accepted for publication March 22, 2004.

Address for reprints: Hiroaki Nomori, MD, PhD, Department of Thoracic Surgery, Saiseikai Central Hospital, 1-4-17 Mita, Minato-ku, Tokyo 108-0073, Japan (E-mail: hnomori@qk9.so-net.ne.jp).

J Thorac Cardiovasc Surg 2004;128: 396-401

0022-5223/$30.00

doi:10.1016/j.jtcvs.2004.03.020

Recent advances in low-dose helical computed tomography (CT) and video-assisted thoracoscopic surgery have enabled the diagnosis of lung cancers while still small in size.[1-6] Although limited resection procedures, such as lung wedge resection or segmentectomy, can cure some clinical T1 N0 M0 non–small cell lung cancers (NSCLCs),[7,8] lymph node metastases are still found in approximately 20% of clinical T1 N0 M0 lung adenocarcinomas.[9-11] Even for patients with pathologic T1 N0 M0 NSCLCs, tumor involvement of intratumoral vessels or the pleura can also cause local recurrence after limited resection because of the spread of tumor cells into lymphatic vessels outside the primary tumor. To predict which T1 N0 M0 lung adenocarcinomas are curable with limited resection from CT findings, several reports have evaluated the importance of ground-glass opacity (GGO) within tumors, usually indicating bronchioloalveolar carcinoma–like spread because adenocarcinomas with GGO appearance are more frequently N0 stage and have less tumor involvement of intratumoral vessels or pleura than those with a solid appearance.[12,13] The criteria of defining GGO appearance on CT scans are subjective, however, potentially leading to erroneous selection of limited surgical intervention.

In recent years, fluorodeoxyglucose (FDG) positron emission tomography (PET) has been used to evaluate pulmonary nodules and tumor stages. It has been reported that FDG uptake correlates with the proliferative activity of tumors[14,15] and is an independent prognostic factor,[16,17] particularly in lung adenocarcinoma. The prognosis in lung adenocarcinoma is known to depend on not only tumor stage but also tumor involvement of intratumoral vessels or pleura.[9,10,18] To predict lymph node metastases and tumor involvement of intratumoral vessels or pleura in clinical T1 N0 M0 lung adenocarcinomas, we measured FDG uptake to determine any correlation with lymph node metastases, lymphatic and vascular invasion, and pleural involvement.

Materials and Methods

Patients

From December 2001 through October 2003, prospective FDG-PET and CT scans were performed for 223 noncalcified pulmonary nodules. Of these, 93 nodules were malignant tumors less than 3 cm in diameter on CT. Clinical TNM stage was determined by using both CT and PET scanning. Of the 93 malignant nodules, 48 were clinical T1 N0 M0 adenocarcinomas of the lung, and these underwent major lung resection with mediastinal lymph node dissection. We excluded 4 adenocarcinomas less than 1 cm in diameter that were PET negative because the spatial resolution of the current generation of PET scanners is 0.7 to 0.8 cm, making it difficult to image pulmonary nodules of less than 1 cm. As a result, we studied 44 adenocarcinomas that were clinically staged as T1 N0 M0 of sizes from 1 to 3 cm. The medical record of each patient was examined with regard to age, sex, maximum tumor diameter, serum level of carcinoembryonic antigen (CEA; <5 ng/mL vs ≥5 ng/mL), operative procedure, pathologic TNM stage, vascular or lymphatic invasion within tumors (positive vs negative), pleural involvement (p0 vs p1 to p3), and grade of histologic differentiation. To identify tumor involvement of the intratumoral vessels or pleura, we routinely conducted elastica-van Gieson staining. Pleural involvement was classified as p0, p1, p2, or p3; that is, a p0 tumor did not extend beyond the elastic pleural layer, a p1 tumor invaded the visceral pleural elastic layer but did not reach the pleural surface, a p2 tumor included tumor exposure on the pleural surface, and a p3 tumor invaded the parietal pleura or chest wall. The tumor stages were based on the TNM classification of the International Union Against Cancer[19]: p2 tumors were classified as T2; p3 tumors were classified as T3; and tumors with intrapulmonary metastasis within the same lobe were classified as T4. Grades of histologic differentiation were classified as well, moderately, or poorly differentiated.

FDG-PET Scanning

Patients were instructed to fast for at least 4 hours before intravenous administration of fluorine 18–tagged FDG. The dosage of fluorine 18–tagged FDG administered was 125 μCi/kg (4.6 MBq/kg) of body weight for nondiabetic patients and 150 μCi/kg (5.6 MBq/kg) of body weight for diabetic patients. PET imaging was performed approximately 60 minutes after administration of FDG with a POSICAM.HZL mPOWER (Positron Co, Houston, Tex). No-attenuation-corrected emission scans were initially obtained in 2-dimensional, high-sensitivity mode for 4 minutes per bed position and taken from the vertical skull through to the midthighs. Immediately thereafter, a 2-bed-position attenuation-corrected examination was performed, with 6 minutes for the emission sequence and 6 minutes for the transmission sequence at each bed position. The images were usually reconstructed in a 256 × 256 matrix by using ordered subset expectation maximization corresponding to a pixel size of 4 × 4 mm, with section spacing of 2.66 mm.

PET Data Analysis

The FDG-PET data were evaluated semiquantitatively on the basis of the contrast ratio (CR) obtained as follows. The regions of interest (ROIs) were placed in the nodules and contralateral lung. Highest activities in the tumor ROI (T) and in the contralateral normal lung ROI (N) were measured. The CR was calculated by using the formula $(T - N)/(T + N)$ in each nodule as an index of FDG uptake. After correction for radioactive decay, the ROIs were also analyzed by computing the standard uptake value (SUV), which was calculated on the basis of the following equation: Tumor activity concentration/Injected dose/Body weight. The maximum SUV within the selected ROIs was also measured and compared with the results of CR.

Statistical Analysis

All data were analyzed for significance by using the 2-tailed Student t test. All values in the text and tables are given as means ± SD.

GTS

TABLE 1. Tumor involvements and pathologic TNM stage for each CR value

CR of FDG uptake	Total lesions	>T1 N0 M0*	Lymphatic invasion	Vascular invasion	Pleural involvement
0.3	16	0	5	1	1
0.4	19	0	5	1	1
0.5†	22	0	5	1	1
0.6	29	2	9	2	2
0.7	37	4	14	7	6
0.8	39	4	15	8	6
0.9	43	8	19	10	8
1.0	44	8	19	10	8

*Pathologically more advanced stages than T1 N0 M0. Three of the 8 cases were p2; the other 5 were p1.
†Cutoff value of CR.

TABLE 2. PET findings and patients' characteristics, tumor size, and serum level of CEA

	CR of FDG uptake		P
	<0.5 (n = 22)	≥0.5 (n = 22)	value
Age (y, mean ± SD)	63 ± 11	64 ± 13	NS
Male (No.)	14	10	NS
Female (No.)	8	12	
Tumor size (cm, mean ± SD)	1.9 ± 0.6	2.2 ± 0.4	NS
CEA (ng/mL)			.001
<5.0	22	10	
≥5.0	0	12	

NS, Not statistically significant.

TABLE 3. Correlation between PET findings and pathologic tumor stage

		CR of FDG uptake	
Pathologic TNM	Total (n = 44)	<0.5 (n = 22)	≥0.5 (n = 22)
T1 N0 M0	36	22*	14*
T1 N1 M0	3	0	3
T2 N0 M0	3	0	3
T4 N0 M0	2	0	2

T2 is classified from pleural involvement grade, p2. T4 is classified from intrapulmonary metastasis.
*Significant difference in the frequency of T1 N0 M0 between the CR <0.5 and CR ≥0.5 groups ($P = .002$).

Results

The pathologic tumor stage was T1 N0 M0 in 36 patients and more advanced in 8 patients (ie, T1 N1 M0 in 3 patients, T2 N0 M0 in 3 patients, and T4 N0 M0 in 2 patients). Lymphatic or vascular invasion within tumors and pleural involvement was seen in 19, 10, and 8 patients, respectively. Table 1 shows the various CR values with relation to the pathologic tumor stage, lymphatic and vascular invasion, and pleural involvement. Although all adenocarcinomas with a CR of less than 0.5 were pathologically staged as T1 N0 M0, some adenocarcinomas with a CR of 0.5 or greater were more advanced than T1 N0 M0, with more frequent lymphatic and vascular invasion and pleural involvement than the former. Therefore medical records were compared between the 22 adenocarcinomas with a CR of less than 0.5 and the 22 adenocarcinomas with a CR of 0.5 or greater.

The maximum SUVs ranged from 0.5 to 3.1 (mean, 1.1 ± 0.7) in the 22 adenocarcinomas with a CR of less than 0.5 and from 1.9 to 8.5 (mean, 3.9 ± 1.8) in the 22 adenocarcinomas with CRs of 0.5 or greater, with the difference between the 2 groups being significant ($P < .001$). Two (9%) of the 22 adenocarcinomas with CRs of less than 0.5 showed an SUV of 2.5 or greater, however, both of which were pathologically staged as T1 N0 M0 and had no involvements of intratumoral vessels or pleura. Seven (32%) of the 22 adenocarcinomas with CRs of 0.5 or greater had SUVs of less than 2.5, of which 2 had a more advanced tumor stage than T1 N0 M0, 6 had lymphatic invasion, and 1 had vascular invasion.

Table 2 shows the results of PET findings with patients' characteristics, tumor size, and serum level of CEA. None of the adenocarcinomas with CRs of less than 0.5 had increased serum levels of CEA, which was significantly less frequent than the incidence of increased CEA in the 12 (55%) of 22 adenocarcinomas with CRs of 0.5 or greater ($P < .001$). There was no significant difference between the 2 groups in mean age, sex ratio, or tumor size.

Table 3 shows the correlation between PET findings and pathologic tumor stage. All adenocarcinomas (100%) with CRs of less than 0.5 were staged as T1 N0 M0. Adenocarcinomas with CRs of 0.5 or greater were staged as T1 N0 M0 in 14 (64%) patients, T1 N1 M0 in 3 patients, T2 N0 M0 caused by p2 (tumor exposure on the pleural surface) in 3 patients, and T4 N0 M0 caused by intrapulmonary metastases in 2 patients. Adenocarcinomas with CRs of less than 0.5 were more likely to be pathologic T1 N0 M0 stage than those with CRs of 0.5 or greater ($P = .002$).

Table 4 shows the correlation between PET findings and lymphatic and vascular invasion within tumors and pleural involvement. Lymphatic invasion was seen in 5 (23%) of 22 adenocarcinomas with CRs of less than 0.5, which was significantly less frequent than 14 (64%) of 22 with CRs of 0.5 or greater ($P = .006$). Vascular invasion was seen in 1 (5%) of 22 adenocarcinomas with CRs of less than 0.5, which was significantly less frequent than 9 (41%) of 22 with CRs of 0.5 or greater ($P = .004$). Pleural involvement was seen in 1 (5%) of 22 adenocarcinomas with CRs of less than 0.5, which was significantly less frequent than 7 (32%) of 22 with CRs of 0.5 or greater ($P = .02$).

Table 5 shows the correlation between PET findings and the histologic degree of differentiation. In the adenocarcinomas with CRs of less than 0.5, well-differentiated and

TABLE 4. Correlation between PET findings and tumor involvement into intratumoral vessels or pleura

Tumor involvement	CR of FDG uptake <0.5 (n = 22)	CR of FDG uptake ≥0.5 (n = 22)	P value
Lymphatic invasion			.006
Yes	5	14	
No	17	8	
Vascular invasion			.004
Yes	1	9	
No	21	13	
Pleural involvement			.02
p0	21	15	
p1-p2	1	7	

TABLE 5. Correlation between PET findings and grade of histologic differentiation of adenocarcinomas

Grade of differentiation	Total (n = 44)	CR of FDG uptake <0.5 (n = 22)	CR of FDG uptake ≥0.5 (n = 22)
Well differentiated	23	19*	4*
Moderately differentiated	17	3	14
Poorly differentiated	4	0	4

There was significant difference in frequency of well-differentiated adenocarcinomas between the CR <0.5 and CR ≥0.5 groups ($P < .001$).

TABLE 6. Correlation between PET findings and tumor stages, tumor involvement of intratumoral vessels, and tumor involvement of pleura in well-differentiated adenocarcinomas

Tumor stage and invasiveness	CR of FDG uptake >0.5 (n = 19)	CR of FDG uptake ≥0.5 (n = 4)	P value
TNM stage			<.01
T1 N0 M0	19	2	
>T1 N0 M0	0	2	
Lymphatic invasion			<.001
Yes	3	4	
No	16	0	
Vascular invasion			.02
Yes	1	2	
No	18	2	
Pleural involvement			<.01
p0	19	2	
p1-p2	0	2	

moderately differentiated adenocarcinomas were seen in 19 and 3 patients, respectively. In the adenocarcinomas with CRs of 0.5 or greater, well-differentiated, moderately differentiated, and poorly differentiated adenocarcinomas were seen in 4, 14, and 4 patients, respectively. Adenocarcinomas with CRs of less than 0.5 were more commonly well differentiated than those with CRs of 0.5 or greater ($P < .001$).

Table 6 shows the PET findings in well-differentiated adenocarcinomas with relation to the tumor stages and tumor involvements. Of the 4 well-differentiated adenocarcinomas with CRs of 0.5 or greater, each one (25%) was a pathologic T1 N1 M0 and T4 N0 M0 carcinoma, respectively; 4 (100%) had lymphatic invasion; 2 (50%) had vascular invasion; and 2 (50%) had pleural involvement. The well-differentiated adenocarcinomas with CRs of 0.5 or greater had advanced tumor stages, lymphatic and vascular invasion, and pleural involvement more frequently than those with CRs of less than 0.5 ($P < .01$, $P < .001$, $P = .02$, and $P < .01$, respectively).

Discussion

Although a criterion for diagnosing pulmonary malignancy with FDG-PET has frequently used an SUV with a cutoff value of 2.5,[20] some authors used visual evaluation, such as comparison of FDG uptake between nodules and mediastinal uptake.[21] The present study evaluated FDG uptake with CR instead of SUV for the following reasons: (1)hyperglycemia in diabetic patients decreases both the blood clearance of FDG and the accumulation of FDG in tumor tissue, and (2) SUV could be different between fat and thin patients because it is measured by using a body weight. Actually, the mean SUV of malignant pulmonary nodules has been reported to be various, ranging from 5.5 to 10.1.[22-25] In breast cancer, Wahl and coworkers[26] have demonstrated that a CR between tumor and contralateral normal breast is a reliable indicator for diagnosing malignancy. We accordingly used CR in the present study and determined that the cutoff value to differentiate between aggressive and nonaggressive adenocarcinomas was 0.5, with which we could differentiate the degree of tumor aggressiveness more accurately than with SUV.

The important points of the present study are as follows. Compared with adenocarcinomas with CRs of 0.5 or greater, those with CRs of less than 0.5 (1) did not show an increased serum level of CEA, (2) did not have lymph node metastases, (3) had less tumor involvement of vessels or pleura, and (4) were more frequently well-differentiated adenocarcinomas. The serum level of CEA in lung adenocarcinomas has been reported to be higher in N1 or N2 disease than in N0 disease.[27] FDG uptake in lung adenocarcinomas is known to often be negative in well-differentiated adenocarcinomas.[28] It has been also reported that well-differentiated adenocarcinomas are more commonly N0 stage and have less tumor involvement of vessels or pleura than moderately or poorly differentiated lesions.[9,12,13,18] Our results agree with those of these earlier studies. There were, however, 4 well-differentiated adenocarcinomas with CRs of 0.5 or greater that had more tumor aggressiveness than the 19 well-differentiated lesions with CRs of less than 0.5. We therefore consider that an FDG

uptake on PET can predict lymph node metastases and tumor invasiveness more accurately than the grade of histologic differentiation in clinical T1 N0 M0 adenocarcinomas.

Although limited resection could be a reasonable approach for T1 N0 M0 lung cancers, it has been reported that lymph node metastases are found in about 20% of clinical T1 N0 M0 adenocarcinomas.[9-11] In 1995, the Lung Cancer Study Group reported the results of a randomized control trial comparing limited resection and lobectomy for clinical T1 N0 M0 NSCLCs.[29] This trial demonstrated the inferiority of limited resection in terms of local relapse and prognosis because some patients actually had pathologic N1 or N2 disease. This is also because tumor involvement of intratumoral vessels or the pleura can cause local recurrence after limited resection, even for pathologic N0 disease, because of the spread of tumor cells into lymphatic vessels outside the primary tumor.[30] The present study showed that clinical T1 N0 M0 adenocarcinomas with CRs of less than 0.5 usually did not metastasize to the lymph nodes and seldom invaded the intratumoral vessels or pleura. This type of lung adenocarcinoma can be cured by means of limited surgical resection, such as segmentectomy or wedge resection. Although it has been reported that NSCLCs of less than 2 cm in size can be cured by means of segmentectomy with mediastinal lymph node dissection (ie, extended segmentectomy),[7] the indication of the extended segmentectomy could be expanded for adenocarcinomas with CRs of less than 0.5 that are less than 3 cm in size.

Mediastinal lymph node dissection is a useful procedure to secure complete local control of an NSCLC, with a subsequent improvement in both survival and nodal staging.[11] However, to minimize the damage caused by mediastinal node dissection in the patients with clinical stage I NSCLC, several authors reduced the dissection of some mediastinal lymph nodal stations with respect to the location of the primary tumor (ie, that the inferior and superior mediastinal lymph node stations could be reduced in the upper lobectomy and lower lobectomy, respectively).[31,32] To expand the possibility of reduction of mediastinal lymph node dissection, a successful intraoperative sentinel lymph node biopsy has been reported.[33,34] The present study showed that lymph node dissection could be reduced for clinical T1 N0 M0 adenocarcinomas with CRs of less than 0.5, without using the sentinel lymph node biopsy.

Although FDG-PET is well known to be useful for tumor staging in lung cancer, we believe that it can also predict lymph node metastases and tumor invasiveness in clinical T1 N0 M0 lung adenocarcinomas. Limited lung resection could be indicated, lymph node dissection or mediastinoscopy could be reduced, or both in this type of adenocarcinoma.

References

1. Kaneko M, Eguchi K, Ohmatsu H, et al. Peripheral lung cancer: screening and detection with low-dose spiral CT versus radiography. *Radiology*. 1996;201:798-802.
2. Yankelevitz DF, Gupta R, Zhao B, Henschke CI. Small pulmonary nodules: evaluation with repeat CT-preliminary experience. *Radiology*. 1999;212:561-6.
3. Henschke CI, Yankelevitz DF. CT screening for lung cancer. *Radiol Clin North Am*. 2000;38:487-95.
4. Nomori H, Horio H, Fuyuno G, Kobayashi R, Morinaga S, Suemasu K. Lung adenocarcinomas diagnosed by open or thoracoscopic vs. bronchoscopic biopsy. *Chest*. 1998;114:40-4.
5. Nomori H, Horio H. Colored collagen is a long-lasting point marker for small pulmonary nodules in thoracoscopic operations. *Ann Thorac Surg*. 1996;61:1070-3.
6. Nomori H, Horio H, Naruke T, Suemasu K. Fluoroscopy-assisted thoracoscopic resection of lung nodules marked with lipiodol. *Ann Thorac Surg*. 2002;74:170-3.
7. Yoshikawa K, Tsubota N, Kodama K, Ayabe H, Taki T, Mori T. Prospective study of extended segmentectomy for small lung tumors. *Ann Thorac Surg*. 2002;73:1055-9.
8. Kodama K, Doi O, Higashiyama M, Yokouchi H. Intentional limited resection for selected patients with T1 N0 M0 non-small cell lung cancer. *J Thorac Cardiovasc Surg*. 1997;114:347-53.
9. Suzuki K, Nagai K, Yoshida J, Nishimura M, Nishizaki Y. Predictors of lymph node and intrapulmonary metastasis in clinical stage IA non-small cell lung carcinoma. *Ann Thorac Surg*. 2001;72:352-6.
10. Asamura H, Nakayama H, Kondo H, Tsuchiya R, Shimosato Y, Naruke T. Lymph node involvement, recurrence, and prognosis in resected small, peripheral, non-small cell lung carcinomas: are these carcinomas candidates for video-assisted lobectomy? *J Thorac Cardiovasc Surg*. 1996;111:1125-34.
11. Naruke T, Goya T, Tsuchiya R, Suemasu K. The importance of surgery of non-small cell carcinoma of lung with mediastinal lymph node metastasis. *Ann Thorac Surg*. 1998;46:603-10.
12. Suzuki K, Asamura H, Kusumoto M, Kondo H, Tsuchiya R. Early peripheral lung cancer: prognostic significance of ground glass opacity on thin-section computed tomographic scan. *Ann Thorac Surg*. 2002;74:1635-9.
13. Matsuguma H, Yokoi K, Anraku M, et al. Proportion of ground-glass opacity on high-resolution computed tomography in clinical T1 N0 M0 adenocarcinoma of the lung: a predictor of lymph node metastasis. *J Thorac Cardiovasc Surg*. 2002;124:278-84.
14. Higashi K, Ueda Y, Yagishita M, et al. FEG PET measurement of the proliferative potential of non-small cell lung cancer. *J Nucl Med*. 2000;41:85-92.
15. Vesselle H, Schmidt RA, Pugsley JM, et al. Lung cancer proliferation correlates with [F-18]fluorodeoxyglucose uptake by positron emission tomography. *Clin Cancer Res*. 2000;6:3837-44.
16. Ahuja V, Coleman RE, Herndon J, Patz EF. The prognostic significance of fluorodeoxyglucose positron emission tomography imaging for patients with non-small cell lung carcinoma. *Cancer*. 1998;83:918-24.
17. Vansteenkiste JF, Stroobants SG, Dupont PJ, et al. Prognostic importance of the standardized uptake value on ^{18}F-fluoro-2-deoxy-glucose-positron emission tomography in non-small cell lung cancer: an analysis of 125 cases. *J Clin Oncol*. 1999;17:3201-6.
18. Noguchi M, Morikawa A, Kawasaki M, et al. Small adenocarcinoma of the lung. Histologic characteristics and prognosis. *Cancer*. 1995;75:2844-52.
19. Sobin LH, Wittekind Ch, editors. UICC: TNM classification of malignant tumours. 6th ed. New York: John Wiley & Sons; 2002. p. 99-103.
20. Coleman RE. PET in lung cancer. *J Nucl Med*. 1999;40:814-20.
21. Marom EM, Sarvis S, Herndon JE, et al. T1 lung cancers: sensitivity of diagnosis with fluorodeoxyglucose PET. *Radiology*. 2002;223:453-9.
22. Dewan NA, Gupta NC, Redepenning LS, et al. Diagnostic efficacy of PET-FDG imaging in solitary pulmonary nodules. *Chest*. 1993;104:997-1002.
23. Gupta NC, Maloof J, Gunel E. Probability of malignancy in solitary

pulmonary nodules using fluorine-18-FDG and PET. *J Nucl Med.* 1996;37:943-8.
24. Imdahl A, Jenkner S, Brink I, et al. Validation of FDG positron emission tomography for differentiation of unknown pulmonary lesions. *Eur J Cardiothorac Surg.* 2001;20:324-9.
25. Lowe VJ, Fletcher JW, Gobar L, et al. Prospective investigation of positron emission tomography in lung nodules. *J Clin Oncol.* 1998; 16:1075-84.
26. Wahl RL, Cody RL, Hutchins GD, et al. Primary and metastatic breast carcinoma: initial clinical evaluation with PET with the radiolabeled glucose analogue 2-[F-18]-fluoro-2-deoxy-D-glucose. *Radiology.* 1991;179:765-70.
27. Takamochi K, Nagai K, Yoshida J, et al. Pathologic N0 status in pulmonary adenocarcinoma is predictable by combining serum carcinoembryonic antigen level and computed tomographic findings. *J Thorac Cardiovasc Surg.* 2001;122:325-30.
28. Higashi K, Ueda Y, Seki H. F-18 FDG PET imaging is negative in bronchiolo-alveolar lung carcinoma. *J Nucl Med.* 1998;39:1016-20.
29. Ginsberg RJ, Rubinstein LV. Randomized trial of lobectomy versus limited resection for T1N0 non-small cell lung cancer. Lung Cancer Study Group. *Ann Thorac Surg.* 1995;60:615-22.
30. Ichinose Y, Yano T, Yokoyama H, Inoue T, Asoh H, Katsuda Y. The correlation between tumor size and lymphatic vessel invasion in resected peripheral stage I non-small cell lung cancer. A potential risk of limited resection. *J Thorac Cardiovasc Surg.* 1994;108:684-6.
31. Naruke T, Tsuchiya R, Kondo H, Nakayama H, Asamura H. Lymph node sampling in lung cancer: how should it be done? *Eur J Cardiothorac Surg.* 1999;16(suppl):S17-24.
32. Asamura H, Nakayama H, Kondo H, Tsuchiya R, Naruke T. Lobe-specific extent of systemic lymph node dissection for non-small cell lung carcinomas according to a retrospective study of metastases and prognosis. *J Thorac Cardiovasc Surg.* 1999;117:1102-11.
33. Liptay MJ, Masters GA, Winchester DJ, et al. Intraoperative radioisotope sentinel lymph node mapping in non-small cell lung cancer. *Ann Thorac Surg.* 2000;70:384-90.
34. Nomori H, Horio H, Naruke T, Orikasa H, Yamazaki K, Suemasu K. Use of technetium-99m tin colloid for sentinel lymph node identification in non-small cell lung cancer. *J Thorac Cardiovasc Surg.* 2002; 124:486-92.

Progression of Focal Pure Ground-Glass Opacity Detected by Low-Dose Helical Computed Tomography Screening for Lung Cancer

Ryutaro Kakinuma, MD, Hironobu Ohmatsu, MD, Masahiro Kaneko, MD, Masahiko Kusumoto, MD, Junji Yoshida, MD, Kanji Nagai, MD, Yutaka Nishiwaki, MD, Toshiaki Kobayashi, MD, Ryosuke Tsuchiya, MD, Hiroyuki Nishiyama, MD, Eisuke Matsui, MD, Kenji Eguchi, MD, and Noriyuki Moriyama, MD

Objective: To clarify the progression of focal pure ground-glass opacity (pGGO) detected by low-dose helical computed tomography (CT) screening for lung cancer.

Methods: A total of 15,938 low-dose helical CT examinations were performed in 2052 participants in the screening project, and 1566 of them were judged to have yielded abnormal findings requiring further examination. Patients with peripheral nodules exhibiting pGGO at the time of the first thin-section CT examination and confirmed histologically by thin-section CT after follow-up of more than 6 months were enrolled in the current study. Progression was classified based on the follow-up thin-section CT findings.

Results: The progression of the 8 cases was classified into 3 types: increasing size (n = 5: bronchioloalveolar carcinoma [BAC]), decreasing size and the appearance of a solid component (n = 2: BAC, n = 1; adenocarcinoma with mixed subtype [Ad], n = 1), and stable size and increasing density (n = 1: BAC). In addition, the decreasing size group was further divided into 2 subtypes: a rapid-decreasing type (Ad: n = 1) and a slow-decreasing type (BAC: n = 1). The mean period between the first thin-section CT and surgery was 18 months (range: 7–38 months). All but one of the follow-up cases of lung cancer were noninvasive whereas the remaining GGO with a solid component was minimally invasive.

Conclusions: The pGGOs of lung cancer nodules do not only increase in size or density, but may also decrease rapidly or slowly with the appearance of solid components. Close follow-up until the appearance of a solid component may be a valid option for the management of pGGO.

Key Words: ground-glass opacity, low-dose helical computed tomography screening, lung cancer

(*J Comput Assist Tomogr* 2004;28:17–23)

Focal pure ground-glass opacities (pGGOs), or nodules of the lungs, has become a major concern as low-dose helical computed tomography (CT) screening for lung cancer becomes more widely available, not only in the field of diagnostic imaging,[1–5] but also in the field of limited surgery.[6–10] GGO is a finding on thin-section CT images of the lung which has been described as a hazy, increased attenuation of the lung tissue with preservation of the bronchial and vascular margins. GGO is usually a nonspecific finding that is found in many types of pulmonary disease.[11] However, some investigators have recently reported that most localized pGGOs or focal GGOs are malignant.[1,2,5] Although a few reports have described the evolution of lung cancer using conventional chest CT,[12–14] thin-section CT[15–17] and low-dose screening CT,[18,19] the natural history of peripheral lung cancers that exhibit as pGGO on thin-section CT images detected using low-dose helical CT screening is still unclear.

The purpose of this retrospective study was to clarify the progression of pGGOs, which were not visible on chest radiographs, detected by low-dose helical CT screening examinations performed every 6 months. We evaluated the progression of pGGOs based on the thin-section CT findings obtained during the follow-up after the first thin-section CT.

PATIENTS AND METHODS

Subjects

Between September 1993 and January 2003, low-dose helical CT screening was conducted semiannually in Tokyo by

From the Division of Thoracic Oncology (Drs Kakinuma, Ohmatsu, Yoshida, Nagai, and Nishiwaki), National Cancer Center Hospital East, Tsukiji, Chiba Japan; the Divisions of Endoscopy (Drs Kaneko and Kobayashi), Diagnostic Radiology (Drs Kusumoto and Moriyama), and Thoracic Surgery (Dr Tsuchiya), National Cancer Center Hospital; the Division of Thoracic Surgery (Dr Nishiyama), Social Health Insurance Medical Center, Okubo, Japan; (Dr Matsui); the Anti–Lung Cancer Association, Ichigaya, Japan; and the Division of Internal Medicine (Dr Eguchi), School of Medicine, Tokai University, Isehara, Japan.

This study was supported in part by a Grant-in-Aid for Cancer Research (13-8) from the Ministry of Health, Labor, and Welfare of Japan and by a Grant-in-Aid from the Second-Term Comprehensive 10-Year Strategy for Cancer Control.

Reprints: Ryutaro Kakinuma, MD, National Cancer Center Hospital East, 6-5-1 Kashiwa-no-ha, Kashiwa, Chiba 277-8577, Japan (e-mail: rkaki@east.ncc.go.jp).

the Anti–Lung Cancer Association (ALCA), a for-profit organization for lung cancer screening.[20,21] Each screening consisted of a low-dose helical CT examination, chest radiography, and cytologic sputum studies. During this period, a total of 15,938 low-dose helical CT examinations were performed in 2052 ALCA members. Among the low-dose helical CT examinations, a total of 1566 CT examinations were judged as having abnormal findings requiring further examination. Sixty-seven cases of lung cancer (peripheral-type lung cancer, 61; hilar-type lung cancer, 6) were detected during the ALCA lung cancer screening project. Out of these 67 cases, 51 cases (76%) were pathologic stage IA. The treatments used in the 67 cases were as follows: surgery (n = 55), radiotherapy (n = 5), radiotherapy and chemotherapy (n = 2), chemotherapy (n = 4), and photodynamic therapy (n = 1). Among the patients with peripheral nodules detected by the low-dose helical CT examinations performed every 6 months, the patients with histologically diagnosed nodules exhibiting pGGO larger than 5 mm in diameter at the time of the first thin-section CT and followed-up by thin-section CT for more than 6 months were enrolled in the current study.

CT Scanning Conditions

A TCT900S Superhelix CT scanner (Toshiba Medical Inc., Tokyo, Japan) was used for all of the examinations. Low-dose helical CT screening was performed under the following conditions: 120 kV, 50 mA, beam width of 10 mm, 1 rotation of the x-ray tube per second, and a table speed of 20 mm per second (pitch 2:1). Reconstruction was performed at intervals of 10 mm. The CT images were displayed on a monitor with a window width of 2000 HU and a window level of −700 HU. If newly developed nodules were identified, thin-section CT examinations were performed under the following conditions: 120 kV, 250 mA, beam width of 2 mm, 1 rotation of the x-ray tube per second, and a table speed of 2 mm per second (pitch 1:1). Reconstruction was performed at intervals of 2 mm using a thin-section CT algorithm.

Evaluation of pGGO Progression Patterns

The progression patterns were classified based on changes in the size and density of the pGGOs on the thin-section CT images. The study period was divided into 2 phases: the unidentified phase (ie, the period prior to the first thin-section CT scan) and the follow-up phase (ie, the period after the first thin-section CT scan). CT images of the pGGOs in the unidentified phase were reviewed independently by 4 physicians (R.K., M.K., H.O., K.E.), who are diagnostic experts in chest radiology, and by 1 radiologist (M.K.). CT findings were adopted as positive findings if 3 of more of the doctors agreed. After the independent reviews, we decided by consensus as to how many pGGOs were newly developed or had arisen from inconspicuous nodules during the helical CT screening period. In the follow-up phase, the size of the pGGOs was measured with a pair of calipers on the thin-section CT images obtained during the initial scan and the final scan by consensus of 2 diagnostic experts (R.K., M.K.) to assess doubling time. The size of the lesion was evaluated using measurements that passed through the center of the lesion. Size was defined as the average of the length and width of the lesion. Doubling times were calculated using the Schwartz equation.[22] The density of faint opacities was evaluated visually on the thin-section CT images obtained during the follow-up phase. pGGO was defined as a homogeneous GGO, and mixed GGO was defined as a GGO with a solid component.

Pathologic Classification of Adenocarcinomas

The histologic findings of the adenocarcinomas were classified according to the criteria of the World Health Organization (WHO)[23] and the criteria of Noguchi et al.[24] The classification system for replacement growth patterns developed by Noguchi et al is as follows: type A (localized bronchioloalveolar carcinoma; LBAC), type B (LBAC with foci of collapsed alveolar structure), and type C (LBAC with foci of active fibroblastic proliferation).

RESULTS

Patient Characteristics

Eight patients with pGGOs (6 men and 2 women) were enrolled in the current study (Table 1). The patients ranged in age from 49 to 69 years (mean, 64 years). With regard to smoking history, 3 patients were nonsmokers, 4 were ex-smokers, and 1 was a current smoker. Four of these 8 pGGO patients were not apparent during the initial screening and became apparent during the screening period, and 3 of the other 4 pGGO patients with inconspicuous opacities visible in retrospect during the initial screening became apparent later. In 1 other case, a conspicuous opacity and multiple old tuberculosis lesions were observed during the initial CT screening. The locations of the pGGOs were as follows: right upper lobe (n = 4), right lower lobe (n = 1), left upper lobe (n = 1), and left lower lobe (n = 2).

Clinical Course

The period between the first visible nodule of a pGGO on a thin-section CT image and the first visible opacity on a helical CT screening image when viewed retrospectively ranged from 13 to 46 months (mean, 22 months) (Table 1). The period between the first thin-section CT examination and the surgery ranged from 7 to 39 months (mean, 19 months). The interval between the last thin-section CT examination and surgery ranged from 1 to 98 days (mean, 32 days).

Histology of GGOs

Seven patients had bronchioloalveolar carcinoma (BAC), defined as noninvasive by the WHO classification in 1999, and 1 had an adenocarcinoma with mixed subtypes (Table 1). Based on Noguchi's classification for small adeno-

TABLE 1. Clinical Characteristics and Histology of Ground-Glass Opacities

Case No.	Sex	Age at Detection (Years)	Smoking Index	Development	Lobe	Period Between: First Visible and the First TS-CT (Months)*	Period Between: The First TS-CT and Surgery (Months)*	Period Between: The Last TS-CT and Surgery (Days)	Histology: WHO Classification	Histology: Noguchi Type
1	M	69	1300	New	RU	41	13	1	Ad	C
2	M	69	800 (ex)	New	RU	13	39	36	BAC	B
3	F	66	Non	New	LL	13	14	33	BAC	A
4	M	66	450 (ex)	New	LU	18	26	98	BAC	A
5	F	65	Non	ic	LL	46	28	13	BAC	B
6	M	69	800 (ex)	ic	RU	21	12	13	BAC	A
7	M	49	515 (ex)	ic	RU	14	10	6	BAC	A
8	M	63	Non	c	RL	13	7	57	BAC	B

Non, nonsmoker; ex, ex-smoker; ic, inconspicuous; c, conspicuous; RU, right upper lobe; LU, left upper lobe; LL, left lower-lobe; TS-CT, thin-section CT; BAC, bronchioloalveolar carcinoma; Ad, adenocarcinoma.
*Number of months was rounded.

carcinomas, the pGGOs consisted of 4 cases of type A and 2 cases of type B while the mixed GGOs consisted of 1 case of type B and 1 case of type C (Tables 1, 2). All the lung cancers were diagnosed at pathologic stage IA.

Progression of pGGOs

The period between the first thin-section CT and the final thin-section CT examinations ranged from 6 to 37 months (mean, 17 months) (Table 2). The opacities ranged in size from 6.5 mm to 17 mm (mean, 10 mm) at the time of the first thin-section CT examination and from 7 mm to 16.5 mm (mean, 10.5 mm) at the time of the final thin-section CT examination. The progressions of 8 opacities in the follow-up phase were classified into 3 types: increasing in size (Increasing type, n = 5), decreasing in size and the appearance of a solid component (decreasing type, n = 2), and stable in size and increasing in density (density type, n = 1). In addition, the decreasing type was classified into 2 subtypes: a rapid-decreasing type (case 1, Fig. 1; decrease in size at the time of the 6-month follow-up) and a slow-decreasing type (case 2, Fig. 2; decrease after follow-up for more than 1 year). All but 1 of the follow-up cases were noninvasive, and the remaining GGO with a solid component was judged to be minimally invasive adenocarcinoma because the size of the collapse fibrosis was only 2 mm in diameter (Fig. 1F).

TABLE 2. Thin-Section CT Findings, Progression Types, and Doubling Time of Ground-Glass Opacities

Case No.	Follow-Up Phase with Thin-Section CT: GGO Size (mm) First	GGO Size (mm) Final	Final TS-CT of GGO: Density	Solid	Finding	Progression Type	Period of Follow-Up with TS-CT (Months)*	GGO Doubling Time (Days)
1	17	12	Increasing	+	Mixed	Dec	12	−214
2	14	12	Increasing	+	Mixed	Dec	37	−1680
3	6.5	7.5	Stable	−	Pure	Inc	13	617
4	7	10.5	Stable	−	Pure	Inc	22	383
5	7	7	Increasing	−	Pure	Den	27	—
6	8.5	9.5	Stable	−	Pure	Inc	12	669
7	6.5	9	Stable	−	Pure	Inc	10	216
8	13.5	16.5	Stable	−	Pure	Inc	6	198

CT, computed tomography; GGO, ground-glass opacity; TS-CT, thin-section computed tomography; Inc, increasing; Dec, decreasing; Den, density.
*Number of months was rounded.

TABLE 3. Evolution of Solid Components in Ground-Glass Opacities

Case No.	Follow-Up Phase with TS-CT Solid Size (mm): First TS-CT	Months After the First TS-CT: 6	11	23	36	Doubling Time (Days)
1	0*	8				14*
2	0	—	2	3	7.5	130†

TS-CT, thin-section computed tomography.

*Doubling time of solid component in case 1 was calculated on the assumption that the first size was 0.5 mm.

†Doubling time of solid component in case 2 was calculated based on the sizes between 11 months and 36 months after the first TS-CT.

Doubling Time

The doubling times of the increasing-type opacities ranged from 198 to 669 days (mean ± SD, 417 ± 220 days). The doubling time of the density-type opacity could not be calculated because it did not change in size. For the decreasing-type opacities, the doubling times were calculated based on the sizes of the pGGOs and the solid components, individually. In case 1, the doubling times of the pGGO and the solid component were −214 and 14 days, respectively. In case 2, the doubling times of the pGGO and the solid component were 1680 and 130 days, respectively.

Correlation of Thin-Section CT Images and Pathologic Findings

The pGGO corresponded to the lepidic growth of cancer cells (Fig. 1E), the thickening of the alveolar wall (Fig. 1E), and the collapse of the alveolar space (Fig. 1E). Solid components corresponded not only to the collapse of the alveolar space and fibrosis (Fig. 1F and Fig. 2G), but also to a severe narrowing of the alveolar space (Fig. 1F). With the development of a solid component in case 2, the distance between the surrounding pulmonary veins and the bronchus gradually narrowed (Figs. 2C–F). The same finding was observed in case 1 (Figs. 1C, D).

DISCUSSION

To our knowledge, this study is the first report to describe the progression of pGGOs in minute lung cancers that appeared as new pGGOs during the screening process or arose from inconspicuous minute nodules on low-dose helical CT screening images obtained at 6-month intervals. In addition, the progressions of the pGGOs on the thin-section CT images were classified into 3 types for the first time. Although a few papers have described the natural history of GGOs in pulmonary adenocarcinoma,[4,7,12,15–17] only 1 researcher[15] reported 2 GGOs that decreased in size, but the size reduction occurred in mixed GGOs, not in pGGOs. The rapid decreasing of a pGGO and the appearance of a solid component has not previously been reported.

Radiologic-pathologic correlations revealed that pGGOs on thin-section CT images mainly represent the lepidic growth of adenocarcinomas.[1,3,4,12,15–17] Solid components in the mixed GGOs were caused by the collapse of alveolar spaces or regions of fibrosis[12] and by a severe narrowing of the alveolar space (case 1). The narrowing of the distance between the surrounding pulmonary vessels and the bronchus was caused not only by the collapse of the alveolar space (cases 1 and 2), but also by the development of fibrosis (case 1) in the pGGO lesions. This finding has been termed "vessel convergence."[12,15,17] Based on our observations of the progression from a pure GGO to a mixed GGO in cases 1 and 2, our results also support the stepwise progression of replacement-type adenocarcinoma.[12,15,17]

Although 1 researcher raised serious questions about the concept of 2-year stability implying benignity,[25] pulmonary nodules are generally considered to be benign if they remain the same size or decrease in size over a 2-year observation period.[26,27] However, our results show that stability or reduction in size over a 2-year period does not necessarily indicate benignity. In the case of a pGGO that decreases in size, can the Schwartz equation be applied to a change from a pGGO to a mixed GGO if the area of the GGO decreases? Usually, the Schwartz equation is based on the assumption that constant exponential tumor growth is the basic pattern of neoplastic proliferation.[22] The doubling time for mixed GGOs has been reported to be 457 ± 260 days.[28] However, progression to a mixed GGO in a case where the pGGO decreases in size and a solid component simultaneously appears has not previously been reported. Moreover, the calculation of doubling times for each component in a mixed GGO has never, to the best of our knowledge, been performed prior to the current study. The doubling time for the solid component in case 1 was calculated based on the assumption that the initial size of the solid component was 0.5 mm, this because the thin-section CT images were taken not only by the single-slice CT scanner described above, but by a multislice CT scanner with the imaging parameters set at 0.5 mm × 4 rows and image reconstruction performed at 1-mm intervals.

Whether pGGOs should be resected or followed up is controversial. Definite evidence of the natural history of pGGOs does not exist at present. However, based on the indirect corroboration described below, we suggest that close follow-up until the appearance of a solid component may be a valid option for the management of pGGO. First, most pGGOs are either atypical adenomatous hyperplasia (preinvasive lesions according to the 1999 WHO criteria), BAC (a noninvasive lesion), or minimally invasive adenocarcinoma.[1,8,29] Second, 1 researcher[7] has previously reported information concerning

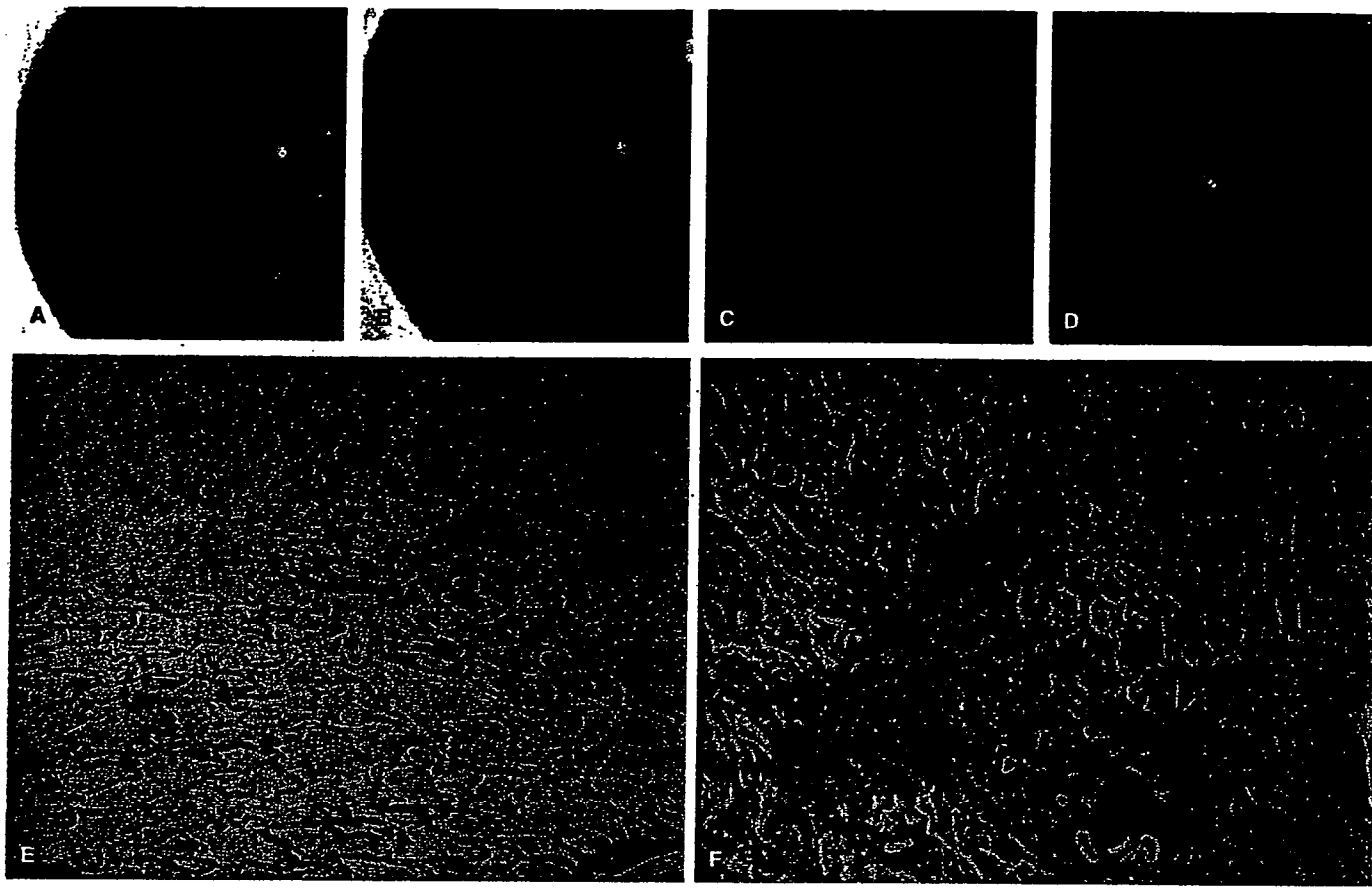

FIGURE 1. Case 1: Adenocarcinoma in a 69-year-old man. A, A faint localized increase in density was identified in segment 1 of the right upper lobe of the lung on a CT screening image obtained in December 2001. B, In retrospect, the opacity was also present on a CT screening image obtained in June 1998. C, Thin-section CT image obtained in December 2001 showing a pGGO in segment 1 of the right upper lobe of the lung. D, Thin-section CT image obtained in June 2002 shows a decrease in the size of the pGGO and the appearance of a solid component. E, Medium-magnification image of the pathologic specimen (H&E staining, ×40). Thickening of the alveolar walls as a result of the tumor cells is visible. F, Medium-magnification image of the pathologic specimen (H&E staining, ×40). Severe narrowing of the alveolar space from the thickening of the alveolar walls and an area of collapse-fibrosis with active fibroblastic proliferation are visible. A right upper lobectomy was performed in January 2003. The lesion was diagnosed as an adenocarcinoma, 17 mm in diameter (Noguchi type C). The size of collapse- fibrosis was 2 mm in diameter.

the natural history of pGGOs after conducting a long-term follow-up study lasting more than 2 years. Five of the 19 cases of pGGOs were diagnosed as lung cancers, that is, 5 BACs (1 case had 2 BACs) and 1 adenocarcinoma, after a mean follow-up of 61 months. Although the patient with adenocarcinoma was followed up for 124 months, personal communication with the author revealed that his lung cancer was of pathologic stage IA and that the size of the central fibrosis of the adenocarcinoma was less than 3 mm in diameter. We have also experienced 2 other pGGOs that developed into mixed GGOs after a 1-year and a 3-year follow-up period, respectively (unpublished data). These lesions were diagnosed as pathologic stage IA adenocarcinomas, and the size of the central fibrosis was 1.5 mm and 2 mm in diameter, respectively. Regarding the relationship between central fibrosis and prognosis, our research team[30] previously reported that 21 out of 100 patients with a lung adenocarcinoma that was 3 cm or less in diameter and which had a central fibrosis of 5 mm or less in diameter had a 5-year survival rate of 100%. Therefore, the adenocarcinoma follow-up cases described above and in this study were thought to be minimally invasive, allowing the possibility of a cure. Third, the adenocarcinoma cases with mixed GGOs did not experience any relapses or deaths, even though the solid components of the GGOs became larger but remained less than 50% of the mixed GGO nodule, this from the standpoint of the GGO's length,[31] the vanishing ratio of GGO[10] ("air-containing type"), and the volume of the GGO.[9] Finally, adenocarcinoma pGGOs tend to grow slowly, as the mean doubling time of pGGOs has been reported to be 813 days[28] or 880 days.[12] In addition, one-fourth of the GGOs in 1 study were

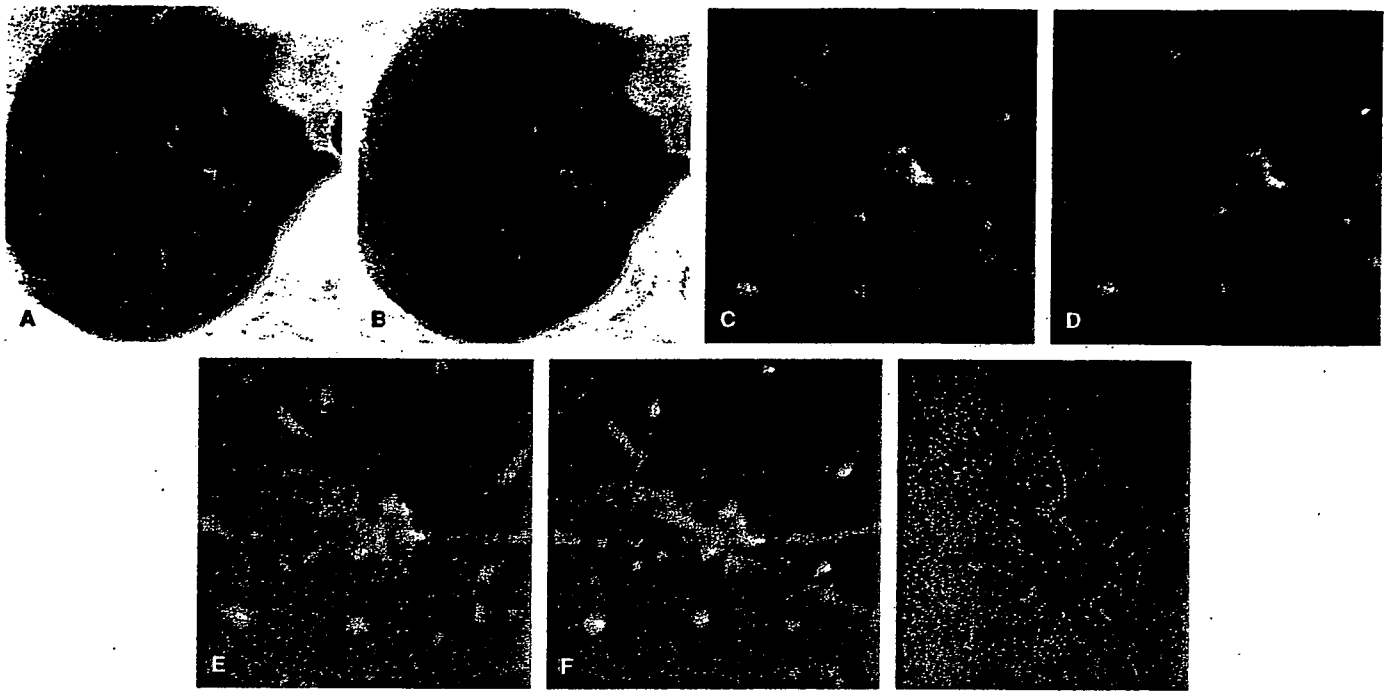

FIGURE 2. Case 2: Bronchioloalveolar carcinoma in a 69-year-old man. A, A faint localized increase in density was identified in segment 1 of the right upper lobe of the lung on a CT screening image obtained in February 1999. B, In retrospect, the opacity was also visible on a CT screening image obtained in February 1998. C, Thin-section CT revealed a pGGO in segment 1 of the right upper lobe of the lung in March 1999. D, Thin-section CT image obtained in February 2000 showing a pGGO with a small solid component. E, Thin-section CT image obtained in February 2001 showing a decrease in the size of the pGGO and a slight increase in the size of the solid component. F, Thin-section CT image obtained in February 2002 showing a larger decrease in the size of the pGGO and an increase in the size of the solid component. G, Low-magnification image of the pathologic specimen (H&E staining, ×5). The foci of alveolar collapse (asterisks) are shown. A right upper lobectomy was performed in May 2002. The lesion was diagnosed as a bronchioloalveolar carcinoma, 15 mm in diameter (Noguchi type B).

stable after a mean follow-up period of 16 months,[17] whereas half of the pGGOs in another study showed no change in size after a median follow-up period of 32 months.[7] Therefore, the classification of some pGGOs may be affected by an overdiagnosis bias.

This study has some limitations. First, the period of pGGO development was not accurately assessed because only thick-sectioned screening CT images were available for the unidentified phase. Therefore, the partial volume effect affected the detectability of small faint opacities on screening CT images. Multislice CT imaging using a narrow collimation and thinner reconstruction images may reveal the natural history of pGGOs more precisely. Second, measurements made with a pair of calipers to calculate doubling times may lead to measurement errors. Although technical advances have been reported,[32,33] we did not have any commercial software for volume measurements. Third, our study cohort was very small. At the start of the helical CT screening project, surgery without follow-up tended to be recommended in cases with pGGO. After knowledge of pGGOs had accumulated (ie, that most pGGOs consisted of preinvasive, noninvasive, or minimally invasive lesions), our treatment procedure changed.[8] Now, resection is only 1 option, not the only option, as in the past. Because of this, resection data cannot always be obtained, and the number of cases was small as a result.

In conclusion, the natural history of pGGOs detected by helical CT screening for lung cancer was partially revealed. A classification for pGGO progression was proposed based on thin-section CT images obtained during the follow-up phase. The pGGOs of lung cancer nodules do not only increase in size or density, but may also decrease rapidly or slowly with the appearance of solid components. Close follow-up until the appearance of a solid component may be a valid option for the management of pGGO.

ACKNOWLEDGMENTS

The authors thank Fumio Shishido, MD, PhD (Department of Radiology, School of Medicine, Fukushima Medical University) for his encouragement. We also wish to thank the pathologists who assisted in this study: Yoshihiro Matsuno, MD (National Cancer Center Research Institute), Tomoyuki Yokose, MD, and Genichiro Ishii, MD (National Cancer Center Research Institute East). We also thank the physicians, the

technical staff, and the administrative staff of the Anti–Lung Cancer Association in Tokyo.

REFERENCES

1. Nakajima R, Yokose T, Kakinuma R, et al. Localized pure ground-glass opacity on high-resolution CT: histologic characteristics. *J Comput Assist Tomogr*. 2002;26:323–329.
2. Nakata M, Saeki H, Takata I, et al. Focal ground-glass opacity detected by low-dose helical CT. *Chest*. 2002;121:1464–1467.
3. Kuriyama K, Seto M, Kasugai T, et al. Ground-glass opacity on thin-section CT: value in differentiating subtypes of adenocarcinoma of the lung. *AJR Am J Roentgenol*. 1999;173:465–469.
4. Yang ZG, Sone S, Takashima S, et al. High-resolution CT analysis of small peripheral lung adenocarcinomas revealed on screening helical CT. *AJR Am J Roentgenol*. 2001;176:1399–1407.
5. Henschke CI, Yankelevitz DF, Mirtcheva R, et al. CT screening for lung cancer: frequency and significance of part-solid and nonsolid nodules. *AJR Am J Roentgenol*. 2002;178:1053–1057.
6. Kodama K, Higashiyama M, Yokouchi H, et al. Prognostic value of ground-glass opacity found in small lung adenocarcinoma on high-resolution CT scanning. *Lung Cancer*. 2001;33:17–25.
7. Kodama K, Higashiyama M, Yokouchi H, et al. Natural history of pure ground-glass opacity after long-term follow-up of more than 2 years. *Ann Thorac Surg*. 2002;73:386–393.
8. Suzuki K, Asamura H, Kusumoto M, et al. "Early" peripheral lung cancer: prognostic significance of ground-glass opacity on thin-section computed tomographic scan. *Ann Thorac Surg*. 2002;74:1635–1639.
9. Matsuguma H, Yokoi K, Anraku M, et al. Proportion of ground-glass opacity on high-resolution computed tomography in clinical T1N0M0 adenocarcinoma of the lung: a predictor of lymph node metastasis. *J Thorac Cardiovasc Surg*. 2002;124:278–284.
10. Kondo T, Yamada K, Noda K, et al. Radiologic-prognostic correlation in patients with small pulmonary adenocarcnomas. *Lung Cancer*. 2002;36:49–57.
11. Austin JM, Muller NL, Friedman PJ, et al. Glossary of terms for CT of the lung: recommendations of the Nomenclature Committee of the Fleischner Society. *Radiology*. 1996;200:327–331.
12. Aoki T, Nakata H, Watanabe H, et al. Evolution of peripheral lung adenocarcinomas: CT findings correlated with histology and tumor doubling time. *AJR Am J Roentgenol*. 2000;174:763–768.
13. White CS, Romney BM, Mason AC, et al. Primary carcinoma of the lung overlooked at CT: analysis of findings in 14 patients. *Radiology*. 1996;199:109–115.
14. Gurney JW. Missed lung cancer at CT: imaging findings in nine patients. *Radiology*. 1996;199:117–122.
15. Koizumi N, Sakai K, Matsuzuki Y, et al. Natural history of cloudy zone of pulmonary adenocarcinoma on HRCT [in Japanese]. *Nippon Igaku Hoshasen Gakkai Zasshi*. 1996;56:715–719.
16. Jang HJ, Lee KS, Kwon OJ, et al. Bronchioloalveolar carcinoma: focal area of ground-glass attenuation at thin-section CT as an early sign. *Radiology*. 1996;199:485–488.
17. Takashima S, Maruyama Y, Hasegawa M, et al. CT findings and progression of small peripheral lung neoplasms having a replacement growth pattern. *AJR Am J Roentgenol*. 2003;180:817–826.
18. Kakinuma R, Ohmatsu H, Kaneko M, et al. Detection failures in spiral CT screening for lung cancer: analysis of CT findings. *Radiology*. 1999;212:61–66.
19. Li F, Sone S, Abe H, et al. Lung cancers missed at low-dose helical CT screening in a general population: comparison of clinical, histopathologic, and imaging findings. *Radiology*. 2002;225:673–683.
20. Kaneko M, Eguchi K, Ohmatsu H, et al. Peripheral lung cancer: screening and detection with low-dose spiral CT versus radiography. *Radiology*. 1996;201:798–802.
21. Sobue T, Moriyama N, Kaneko M, et al. Screening for lung cancer with low-dose helical computed tomography: Anti–Lung Cancer Association project. *J Clin Oncol*. 2002;20:911–920.
22. Schwartz M. A biomathematical approach to clinical tumor growth. *Cancer*. 1961;14:1272–1294.
23. Travis W, Colby T, Corrin B, et al. *Histological Typing of Lung and Pleural Tumors*. Berlin: Springer; 1999.
24. Noguchi M, Morikawa A, Kawasaki M, et al. Small adenocarcinoma of the lung: histologic characteristics and prognosis. *Cancer*. 1995;75:2844–2852.
25. Yankelevitz DF, Henschke CI. Does 2-year stability imply that pulmonary nodules are benign? *AJR Am J Roentgenol*. 1997;168:325–328.
26. Swensen SJ, Jett JR, Hartman TE, et al. Lung cancer screening with CT: Mayo Clinic experience. *Radiology*. 2003;226:756–761.
27. Benjamin MS, Drucker EA, McLoud TC, et al. Small pulmonary nodules: detection at chest CT and outcome. *Radiology*. 2003;226:489–493.
28. Hasegawa M, Sone S, Takashima S, et al. Growth rate of small lung cancers detected on mass CT screening. *Br J Radiol*. 2000;73:1252–1259.
29. Nakata M, Sawada S, Saeki H, et al. Prospective study of thoracoscopic limited resection for ground-glass opacity selected by computed tomography. *Ann Thorac Surg*. 2003;75:1601–1606.
30. Suzuki K, Yokose T, Yoshida J, et al. Prognostic significance of the size of central fibrosis in peripheral adenocarcinoma of the lung. *Ann Thorac Surg*. 2000;69:893–897.
31. Aoki T, Tomoda Y, Watanabe H, et al. Peripheral lung adenocarcinoma: correlation of thin-section CT findings with histologic prognostic factors and survival. *Radiology*. 2001;220:803–809.
32. Yankelevitz Df, Reeves AP, Kostis WJ, et al. Small pulmonary nodules: volumetrically determined growth rates based on CT evaluation. *Radiology*. 2000;217:251–256.
33. Ko JP, Rusinek H, Jacobs EL, et al. Small pulmonary nodules: volume measurement at chest CT-phantom study. *Radiology*. 2003;228:864–870.

Jpn J Clin Oncol 2005;35(11)667–671
doi:10.1093/jjco/hyi177

A Flexible Endoscopic Surgical System: First Report on a Conceptual Design of the System Validated by Experiments

Toshiaki Kobayashi[1], Sean Lemoine[1,2], Akihiko Sugawara[1,2], Takaaki Tsuchida[1], Takuji Gotoda[1], Ichiro Oda[1], Hirohisa Ueda[3] and Tadao Kakizoe[1]

[1]National Cancer Center, [2]Japan Association for the Advancement of Medical Equipment and [3]Pentax Corporation, Tokyo, Japan

Received May 17, 2005; accepted August 25, 2005; published online November 8, 2005

Background: Surgery is a standard diagnostic and therapeutic procedure. However, its technical difficulty and invasiveness pose problems that are yet to be solved even by current surgical robots. Flexible endoscopes can access regions deep inside the body with less invasiveness than surgical approaches. Conceptually, this ability can be a solution to some of the surgical problems.
Methods: A flexible (surgical) endoscopic surgical system was developed consisting of an outer and two inner endoscopes introduced through two larger working channels of the outer endoscope. The concept of the system as a surgical instrument was assessed by animal experiments.
Results: Gastric mucosa of the swine could be successfully resected using the flexible endoscopic surgical system, thereby showing us the prospect and directions for further development of the system.
Conclusion: The concept of a flexible endoscopic surgical system is considered to offer some solutions for problems in surgery.

Key words: surgical robot – endoscopic surgery – surgery – robotics – endoscope

INTRODUCTION

We recently reported a new concept for endoscopic mucosal resection of gastric cancer with the use of a magnetic anchor. The anchor consisted of microforceps and a magnetic weight in order to grasp, stabilize and pull up the gastric mucosa (1). During the experiments, we thought that the procedure would be easier if one more endoscope was present to hold and stabilize the mucosa instead of the magnetic anchor.

Concerning flexible endoscopes, there are some ultrathin endoscopes that can be inserted into the working channels of standard endoscopes, such as gastrointestinal endoscopes. If the outer endoscope is able to contain larger and multiple working channels, several thin endoscopes could be inserted through the outer endoscope. This would allow for the resecting procedures. Such a system could also be applied to the fields where current surgical robots are targeting.

One of the problems with current surgical robots is inaccessibility to regions located deep inside the body, particularly regions reached through narrow and winding routes, such as the digestive tracts and blood vessels. However, some early gastric cancers can be resected endoscopically with much less invasiveness than surgery. These surgeries cannot be performed by current surgical robot systems because those regions were not originally considered places for the systems to operate.

An experimental flexible endoscopic surgical system was developed to cope with these problems of accessibility, consisting of a flexible outer endoscope with two working channels through which two inner flexible endoscopes could be inserted. These inner endoscopes were designed to have similar functions as flexible gastrointestinal endoscopes allowing for performance of standard endoscopic procedures even when introduced through the outer endoscope.

The uses of the flexible endoscopic system as a surgical instrument, as well as its functionality, were confirmed during gastric mucosal resection of the swine. This is in contrast to the current limitations for surgical robotics in terms of lesion access.

MATERIALS AND METHODS

FLEXIBLE SURGICAL ENDOSCOPE

As shown in Fig. 1, the flexible surgical endoscope consists of an outer flexible endoscope and two inner flexible endoscopes inserted into the working channel of the outer endoscope. The specifications of these endoscopes are listed in Table 1.

For reprints and all correspondence: Toshiaki Kobayashi, Cancer Screening Technology Division, Research Center for Cancer Prevention and Screening, National Cancer Center, 1-1, Tsukiji 5-chome, Chuo-ku, Tokyo 104-0045, Japan. E-mail: tkobayas@ncc.go.jp

The outer endoscope also has a 2.8 mm working channel and a charge coupled device (CCD) enabling the endoscope to operate in a similar fashion as standard gastrointestinal endoscopes. The endoscopic images are observed on cathode ray tube (CRT) monitors in the same manner as video-endoscopes.

Each of the inner endoscopes has a 2.0 mm working channel allowing accessories such as forceps and an electrocautery tip to be introduced and used. Unlike the outer endoscope, the inner endoscopes have optic fiber bundles for image visualization, instead of a CCD. These endoscopic images are also observed on CRT monitors. However, a video-adaptor, i.e. a small CCD video camera, must be connected onto each eye piece of the inner endoscopes in order to view the image on the monitors.

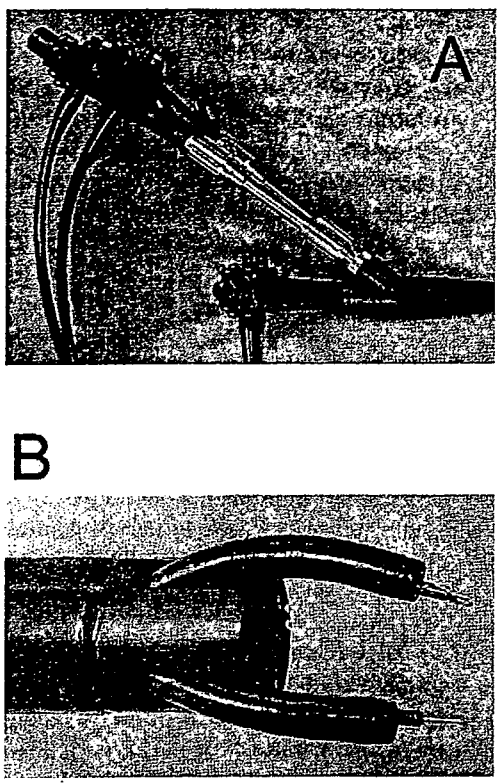

Figure 1. The flexible endoscopic surgical system. (A) The inner endoscope is inserted through a telescopic connecting device, which connects to the opening for the working channel of the outer endoscope near its control section. (B) At the tip of the outer endoscope two inner endoscopes protrude laterally, obtaining a certain distance between the two endoscopes.

Table 1. Specifications of the flexible endoscopic surgical system

	Outer endoscope	Inner endoscope
Total length (mm)	975	1395
Working length (mm)	665	1050
Insertion portion diameter (mm)	20	4.9
Tip bending (degree) (up/down, right/left)	210/120, 120/120	210/120, 120/120
Field of view (degree)	140	120
Depth of field (mm)	4–100	3–50
Channel diameter (mm)	7, 7, 2.8	2

These combined endoscopes are manipulated manually by three physicians together with the help of several assistants. The system, as a whole, operates similar to surgical robotic systems.

PHYSICIANS

Two series of experiments were conducted. The first series was performed by a senior endoscopist and three resident physicians in order to assess the system with consideration to its endoscopic nature. The senior endoscopist was trained within the specialty of internal medicine, whereas one of the resident physicians was in training for internal medicine and the other two were for surgery.

The purpose of the subsequent series was to assess the concept of the flexible surgical endoscope from the viewpoint of surgeons. Consequently, the procedure was performed by two senior endoscopists, one having more than 15 year experience as a surgeon and the other having some surgical training, in addition to two residents who were in training for surgery.

These two series were performed on separate occasions, with none of the physicians performing in both series.

TEST SUBJECT

Three female swine, under intravenous anesthesia, were laid on an examination table in the left lateral position. Within the first experiment, a 35.6 kg and a 34.1 kg swine were used. In the following experiment, a 41.8 kg swine was used. During these experiments, the law for the humane treatment and management of animals was observed.

PROCEDURE

The procedure was similar to standard endoscopic mucosal resection with the exception of one more endoscope for stabilization of the gastric mucosa.

First, an incision was made in the mucosa surrounding the region of stomach intended for resection (2,3). The outer endoscope was inserted through the esophagus into the gastric cavity. Subsequently, using the telescopic connecting devices (Fig. 1), the inner endoscopes were inserted into the working channels of the outer endoscope and introduced into the gastric cavity.

The outer endoscope was placed near the region in which the first incision was made. Thereafter, the resecting procedure was performed using an electrosurgical knife through one of the working channels of the inner endoscopes, whereas the other contained forceps. Within the procedure, the operator decided which side of the working channels would use the electrosurgical knife.

These procedures were observed on three CRT monitors, each of which was connected to its endoscopic counter part.

The resecting procedures were performed on the anterior wall of the gastric angle, the anterior wall of the middle gastric body and the greater curvature of the middle gastric body in the

first series for the assessment of endoscopic features. Within the following series, the resecting procedures were performed on two regions adjacent to the greater curvature of the lower gastric body.

RESULTS

Concerning insertion of the outer endoscope through the esophagus into the gastric cavity, some difficulties were encountered owing to the large diameter of the outer endoscope and the relatively small size of the swine in both experimental series. However, the outer endoscope was introduced into the gastric cavity.

As for insertion of the inner endoscopes through the working channels of the outer endoscope, there were no difficulties experienced, even when the outer endoscope was bent due to insertion through the esophagus. Access to regions of the gastric wall was limited to the greater curvature due to the rigidity of the outer endoscope.

Maneuverability of the flexible endoscopic surgery system was satisfactory regarding the experiments were the first experiences for the physicians involved, despite some problems to solve.

The images from the outer endoscope were similar to those of standard gastrointestinal video-endoscopes due to the CCD system used in the outer endoscope. However, the images from the inner endoscopes were inferior to those of the outer endoscope. This inferiority was attributed to the limited number of optical fibers within the inner endoscope and deterioration of the image caused by conversion from optical images to electrical images through the use of a video-adapter. Consequently, during most of the procedure, endoscopic images were mainly observed using the monitor for the outer endoscope.

Some differences in use of the inner endoscopes for the resecting procedures between the first series and the second series were noticed. In the first series, the physicians appeared to have difficulties in some of the procedures such as accessing the mucosa, stabilization of the mucosal flap and resection procedures. These procedures were considered standard techniques for actual surgery, which means surgical experiences are required even to maneuver the flexible endoscopic surgical system.

Within the second series conducted by endoscopists with surgical experience, the resecting procedures were satisfactory, despite the fact this was their first experience using the system (Fig. 2). Through cooperation between the operator and assistants using verbal commands, manipulation of the inner endoscopes and the outer endoscope could be achieved. The functions of the inner endoscopes could be modified by changing the instruments inserted into the working channels. The flexible nature of the inner endoscopes allowed additional functions such as stabilization of the gastric wall by the longitudinal flank of the endoscope, as shown in Fig. 2C.

Within all the experiments, resecting procedures were completed without any complications such as perforation of the gastric wall. Consequently, five mucosal pieces, with sizes of

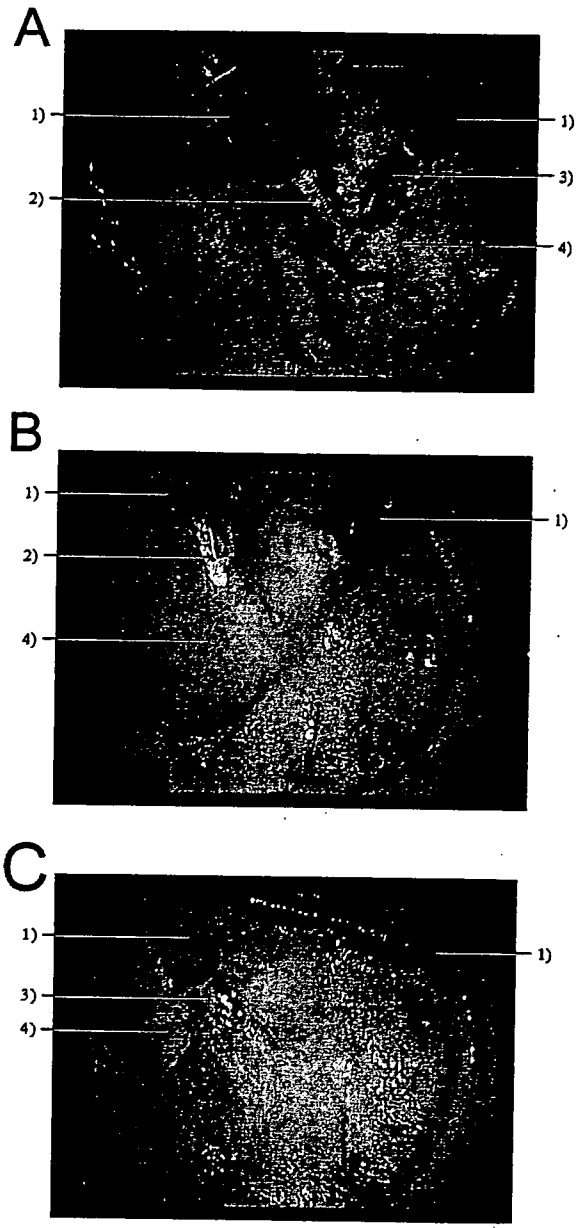

Figure 2. Images of the resecting procedures. (1) Inner endoscope, (2) forceps, (3) electrosurgical knife and (4) mucosal flap. (A) The right inner endoscope, with an electrosurgical knife introduced through its working channel, was maneuvered by the operator. The left inner endoscope, with forceps, was maneuvered by an assistant. (B) The tip of the right inner endoscope is holding up the mucosal flap in order to assist the forceps of the left inner endoscope to grasp the mucosal flap. (C) The right inner endoscope is pulling up the mucosal flap using forceps concealed in this image. In addition, using the flexibility of the endoscope, the gastric wall is stabilized by the longitudinal flank of the inner endoscope.

2.8×1.6 cm^2, 2.8×2.7 cm^2 and 2.6×2.0 cm^2 in the first series, and 3.2×2.7 cm^2 and 4.0×3.4 cm^2 in the second series were each resected in a single piece.

DISCUSSION

Surgical procedures are good options for diagnosis and treatment providing several advantages over non-surgical